

AD-A145 399

ELECTRON TRAPS IN THE GAAS PERMEABLE BASE TRANSISTOR
(U) AIR FORCE INST OF TECH WRIGHT-PATTERSON AFB OH
J L RIENSTRA JUN 84 AFIT/CI/NR-84-41T

1/1

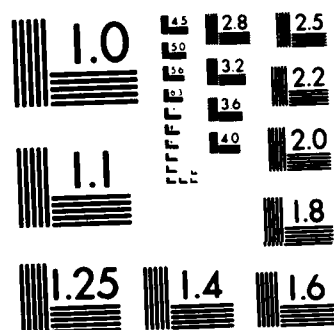
UNCLASSIFIED

F/G 20/12

NL

END

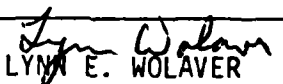
218



MICROCOPY RESOLUTION TEST CHART
NATIONAL BUREAU OF STANDARDS 1963-A

UNCLASS

SECURITY CLASSIFICATION OF THIS PAGE (When Data Entered)

REPORT DOCUMENTATION PAGE		READ INSTRUCTIONS BEFORE COMPLETING FORM
1. REPORT NUMBER	2. GOVT ACCESSION NO.	3. RECIPIENT'S CATALOG NUMBER
AFIT/CI/NR 84-41T		
4. TITLE (and Subtitle)		5. TYPE OF REPORT & PERIOD COVERED
Electron Traps in the GaAs Permeable Base Transistor		THESIS/DISSERTATION
		6. PERFORMING ORG. REPORT NUMBER
7. AUTHOR(s)		8. CONTRACT OR GRANT NUMBER(s)
Jeffrey Lee Rienstra		
9. PERFORMING ORGANIZATION NAME AND ADDRESS		10. PROGRAM ELEMENT, PROJECT, TASK AREA & WORK UNIT NUMBERS
AFIT STUDENT AT: Massachusetts Institute of Technology		
11. CONTROLLING OFFICE NAME AND ADDRESS		12. REPORT DATE
AFIT/NR		June 1984
WPAFB OH 45433		13. NUMBER OF PAGES
		50
14. MONITORING AGENCY NAME & ADDRESS (if different from Controlling Office)		15. SECURITY CLASS. (of this report)
		UNCLASS
		15a. DECLASSIFICATION/DOWNGRADING SCHEDULE
16. DISTRIBUTION STATEMENT (of this Report)		
APPROVED FOR PUBLIC RELEASE; DISTRIBUTION UNLIMITED		
17. DISTRIBUTION STATEMENT (of the abstract entered in Block 20, if different from Report)		
B		
18. SUPPLEMENTARY NOTES		
APPROVED FOR PUBLIC RELEASE: IAW AFR 190-1/		
<div style="text-align: right;">  LYNN E. WOLAVER Dean for Research and Professional Development AFIT, Wright-Patterson AFB OH </div>		
19. KEY WORDS (Continue on reverse side if necessary and identify by block number)		
24 JUN 84		
20. ABSTRACT (Continue on reverse side if necessary and identify by block number)		
ATTACHED		

DD FORM 1 JAN 73 1473

EDITION OF 1 NOV 65 IS OBSOLETE

UNCLASS

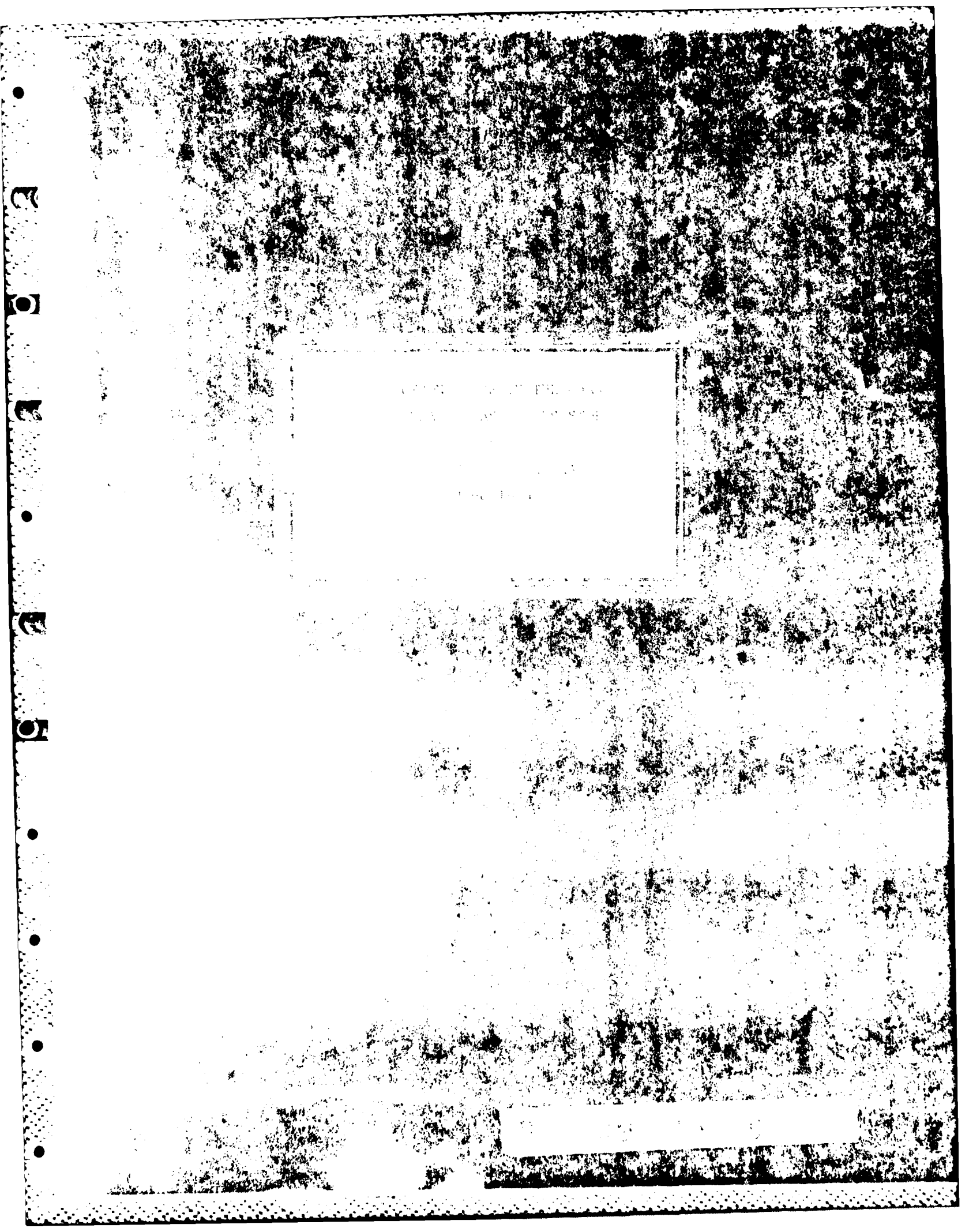
SECURITY CLASSIFICATION OF THIS PAGE (When Data Entered)

84 09 13 034

AD-A145 399

DTIC FILE COPY

DTIC
ELECTE
SEP 13 1984
B



ELECTRON TRAPS IN THE GaAs

PERMEABLE BASE TRANSISTOR

by

JEFFREY LEE RIENSTRA

Submitted to the Department of Physics
on June 4, 1984 in partial fulfillment of the
requirements for the Degree of Master of Science in
Physics

ABSTRACT

An experimental study of deep level traps in the GaAs permeable base transistor (PBT) was carried out using current deep level transient spectroscopy (DLTS). This type of measurement was used because of its ability to detect electron traps in the base region of the PBT, the region most critical to device performance. The automated measurement system was able to capture the PBT current transients and store them for later analysis. With this system, the DLTS signal could be obtained for several rate windows with one thermal scan.

The results of the DLTS measurements indicated a number of different deep level traps in the devices tested. The PBT devices tested were each fabricated in slightly different ways, and the differences in the traps detected were understandable. The forward voltage pulse used to fill the deep level traps was relatively high, and hole traps were observed as well as electron traps. One hole trap which was common to three of the devices is thought to be related to the presence of copper in the GaAs around the base. Another hole trap found in one of the devices is thought to be due to iron.

Thesis Supervisor: Dr. Alan L. McWhorter

Title: Professor of Electrical Engineering

AFIT/NR
Wright-Patterson AFB OH 45433

AUTHOR: Jeffrey Lee Rienstra

1. Did this research contribute to a current Air Force project?

() a. YES () b. NO

() a. YES () b. NO

() a. MAN-YEARS () b. \$

() a. HIGHLY SIGNIFICANT () b. SIGNIFICANT () c. SLIGHTLY SIGNIFICANT () d. OF NO SIGNIFICANCE

NAME	GRADE	POSITION
------	-------	----------

[illegible]

STATEMENT(s):

ELECTRON TRAPS IN THE GaAs
PERMEABLE BASE TRANSISTOR

by

JEFFREY LEE RIENSTRA
B. S., University of North Dakota
(1977)

SUBMITTED IN PARTIAL FULFILLMENT
OF THE REQUIREMENTS OF THE
DEGREE OF

MASTER OF SCIENCE
IN PHYSICS

at the

MASSACHUSETTS INSTITUTE OF TECHNOLOGY

June 1984

© Jeffrey Lee Rienstra 1984

The author hereby grants to M.I.T. permission to reproduce and to distribute copies of this thesis document in whole or in part.

Signature of Author Jeffrey L. Rienstra Department of Physics
June 4, 1984

Certified by Alan L. McWhorter Alan L. McWhorter
Thesis Supervisor

Accepted by _____ George F. Koster
Chairman, Departmental Committee on Graduate Students

ELECTRON TRAPS IN THE GaAs
PERMEABLE BASE TRANSISTOR

by

JEFFREY LEE RIENSTRA

Submitted to the Department of Physics
on June 4, 1984 in partial fulfillment of the
requirements for the Degree of Master of Science in
Physics

ABSTRACT

7 An experimental study of deep level traps in the GaAs permeable base transistor (PBT) was carried out using current deep level transient spectroscopy (DLTS). This type of measurement was used because of its ability to detect electron traps in the base region of the PBT, the region most critical to device performance. The automated measurement system was able to capture the PBT current transients and store them for later analysis. With this system, the DLTS signal could be obtained for several rate windows with one thermal scan.

The results of the DLTS measurements indicated a number of different deep level traps in the devices tested. The PBT devices tested were each fabricated in slightly different ways, and the differences in the traps detected were understandable. The forward voltage pulse used to fill the deep level traps was relatively high, and hole traps were observed as well as electron traps. One hole trap which was common to three of the devices is thought to be related to the presence of copper in the GaAs around the base. Another hole trap found in one of the devices is thought to be due to iron. ✱

Thesis Supervisor: Dr. Alan L. McWhorter

Title: Professor of Electrical Engineering

BIOGRAPHICAL NOTE

The author was born in Valley City, North Dakota on December 9, 1954. He received a B. S. degree in physics from the University of North Dakota in May, 1977 and was commissioned into the United States Air Force. In the fall of 1982 he was admitted to the graduate school at the Massachusetts Institute of Technology under the sponsorship of the Air Force Institute of Technology.



Accession For	
NTIS GRA&I	<input checked="" type="checkbox"/>
DTIC TAB	<input type="checkbox"/>
Unannounced	<input type="checkbox"/>
Justification	
By	
Distribution/	
Availability Codes	
Dist	Avail and/or Special
A-1	

TABLE OF CONTENTS

I. INTRODUCTION.....	7
II. DEEP LEVEL TRANSIENT SPECTROSCOPY.....	14
III. MEASUREMENT APPARATUS.....	27
IV. EXPERIMENTAL RESULTS.....	31
V. DISCUSSION.....	44
VI. SUMMARY.....	50

LIST OF FIGURES

Fig. 1. Cross section of the permeable base transistor.....	9
Fig. 2. Depletion region around base of PBT for three base voltage conditions.....	10
Fig. 3. Three-dimensional view of PBT with broken away region.....	12
Fig. 4. The four basic capture and emission processes.....	15
Fig. 5. Band diagram for Schottky contact under three bias conditions.....	19
Fig. 6. DLTS measurement sequence.....	22
Fig. 7. Dependence of $S(T)$ on temperature.....	23
Fig. 8. Diagram of DLTS measurement system.....	28
Fig. 9. Example of DLTS signal versus temperature.....	37
Fig. 10. Plots for two measured traps and two known traps.....	39
Fig. 11. Dependence of hole trap peak height on fill-up pulse width.....	42

LIST OF TABLES

Table 1.	Summary of differences in fabrication parameters among PBT's tested.....	32
Table 2.	Summary of traps detected.....	33
Table 3.	Parameters E_{na} and σ_{na} for known electron traps.....	35
Table 4.	Parameters E_{pa} and σ_{pa} for known hole traps.....	36
Table 5.	Approximate trap concentrations.....	40
Table 6.	Change in DLTS peak location as base bias changed for Second Chance.....	46

I. INTRODUCTION

The presence of deep level traps can sometimes adversely affect the operation of semiconductor devices. Electron traps in gallium arsenide may affect the operation of the permeable base transistor (PBT) in ways which, as of now, are not clearly understood. The purpose of this research is to investigate electron traps in the PBT through the use of current deep level transient spectroscopy (DLTS). This technique allows the identification of electron traps by means of their characteristic ionization energies and capture cross sections.

This thesis is divided into six chapters. In Chapter I the subject of the thesis is introduced, trap levels are defined, and the PBT is described. Chapter II provides background on the DLTS technique and how it can be applied to the PBT. In Chapter III the DLTS measurement apparatus is described, and in Chapter IV the results of the DLTS measurements are presented and the fabrication parameters of the devices tested are briefly described. The results of the measurements and some of the notable findings are discussed in Chapter V. Finally, the major topics of the thesis are summarized in Chapter VI.

Trap levels, also called deep levels, impurity centers, or defect centers, are energy levels within the band gap of semiconductors caused by impurities or crystal defects which can capture or emit free electrons or holes. Deep level traps are usually distinguished from hydrogenic shallow donor or acceptor levels which are often introduced through intentional doping of the material.¹

The permeable base transistor is a three-terminal semiconductor structure developed by Lincoln Laboratory which has the potential for producing gain at very high frequencies.² The PBT basically consists of a

very fine tungsten grating embedded within a crystal of n-type GaAs. Emitter and collector contacts are located on either side of the tungsten base grating. A cross section of the device is shown in Fig. 1. Under a positive collector-emitter bias electrons flow from the emitter to the collector. To do so, the electrons must pass through the base grating. A voltage applied to the base controls the current by changing the potential barrier experienced by the electron.

The metal base grating in contact with the n-type GaAs forms a Schottky barrier around the base. The periodicity of the grating in the present devices is 3200 \AA , with approximately equal line-to-space ratio so that the spacing between lines is of the order of a few tenths of a micrometer. With typical carrier concentrations the zero-bias depletion width in the GaAs is larger than the spacing between lines, as shown in Fig. 2(a). Therefore, the electrons must overcome a potential barrier as they move from emitter to collector. If a positive voltage is applied to the base metal the potential barrier is lowered as shown in Fig. 2(b), and the emitter current increases. As the base bias is increased further the barrier vanishes in the middle of the gap between the grating lines as shown in Fig. 2(c), and the current becomes limited by the width of the conducting channel between the grating lines.

The fabrication of the PBT involves putting down several patterned layers of semiconductor and metal using a combination of x-ray lithography, photolithography, and etching techniques. The substrates are silicon-doped GaAs. After polishing and etching, a 2- μm sulfur-doped vapor phase epitaxy (VPE) buffer layer is grown, followed by a 4000 \AA active layer with a donor concentration of $5 \times 10^{16} \text{ cm}^{-3}$. Following this, a 300-500 \AA layer of tungsten is deposited, and the base grating with a period of 3200 \AA is

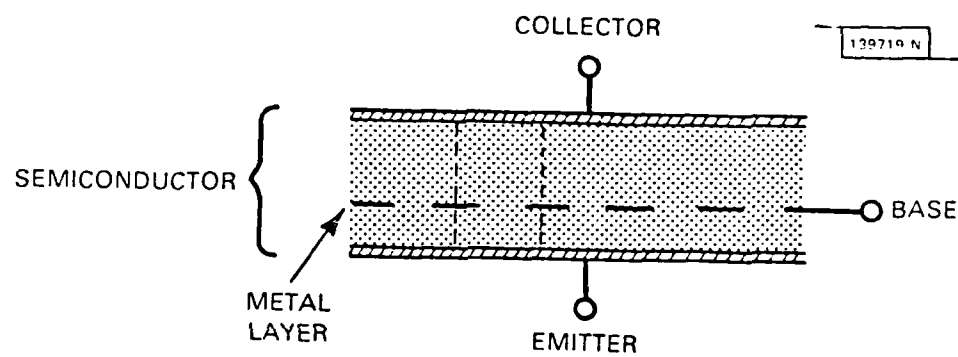
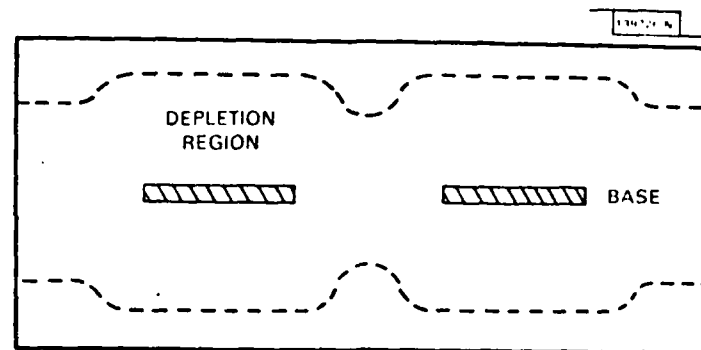
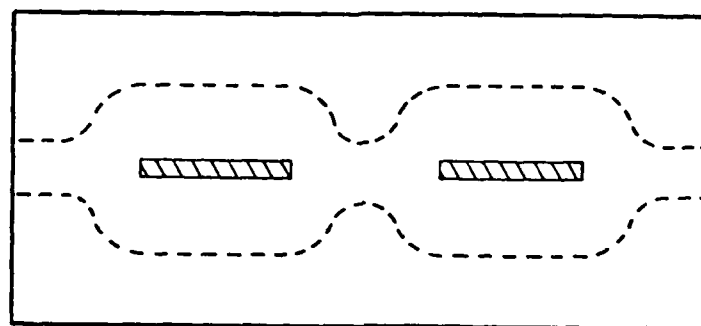


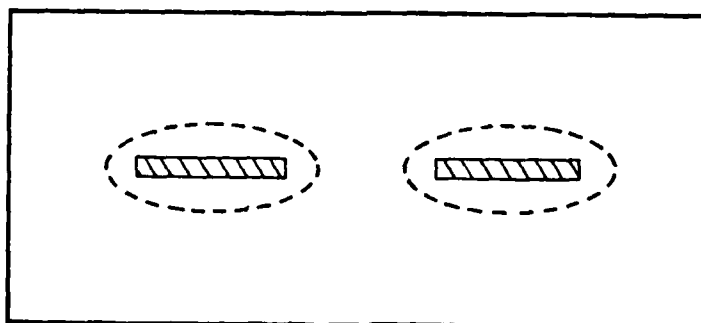
Fig. 1. Cross section of the permeable base transistor.



(a)



(b)

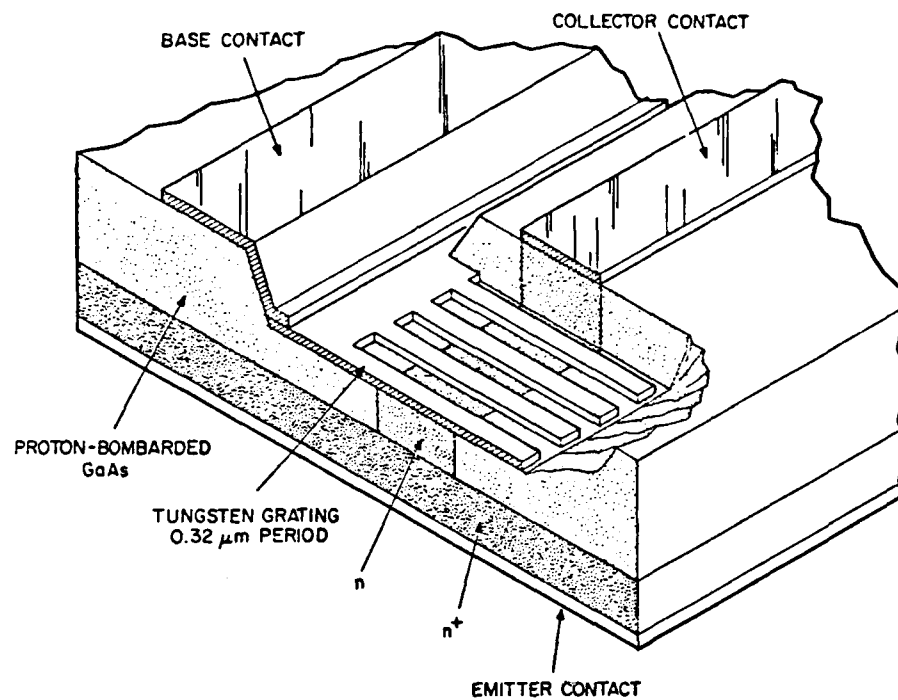


(c)

Fig. 2. Depletion region around base of PBT for three base voltage conditions: (a) zero volts; (b) moderate positive voltage; and (c) more positive voltage.

formed using x-ray lithography and reactive ion etching. After base contact pads are deposited, GaAs is epitaxially grown over the base grating. Following the overgrowth, the base contact pads are opened, and ohmic contacts are formed for the emitter and collector. After protecting the active area of each device with photoresist, protons are implanted to reduce the capacitance between base pads and contact overlay pads. The photoresist is then removed and gold contact overlay pads are formed. After the devices on each wafer are isolated using a chemical etch, they are packaged for testing. A three-dimensional drawing of a PBT with a broken away region is shown in Fig. 3.

In a completed device the width of the depletion region around the base grating depends upon both the voltage applied to the base and the concentration of space charge in the depletion region. The various fabrication processes may introduce deep level traps into the semiconductor material in the region of the base grating. As will be shown in Chapter II, the presence of deep level traps in the depletion region alters the space charge concentration and thus the depletion width. A change in the depletion width in turn affects the collector-emitter current through the PBT by changing the potential barrier in the base region. Since current DLTS measures the effect of deep level traps in the base region, it is well suited to measuring the traps which affect PBT performance. Because of the extremely small dimensions of the grating structure, it is difficult to determine exactly the condition of the semiconductor material after all the device fabrication steps have been completed. Since the collector-emitter current must pass through the base grating, the use of current DLTS enables one to characterize the traps in the most important region of the PBT.



PERMEABLE BASE TRANSISTOR

Fig. 3. Three-dimensional view of PBT with broken away region.

Deep level traps in the PBT may affect the performance of the device in several ways. The presence of impurities increases the amount of ionized impurity scattering and decreases the electron mobility. In addition, the trapping action of the deep levels affects carrier transport, and could decrease the frequency performance of the device. There may also be other effects of deep level traps, not clearly understood, which degrade the performance of the PBT.

II. DEEP LEVEL TRANSIENT SPECTROSCOPY

Deep level transient spectroscopy was introduced by Lang and has since become a very useful tool for characterizing electron and hole traps in semiconductors.³ The technique involves the measurement of the transient response of a p-n or a metal-semiconductor junction due to emission of electrons or holes from trap levels. The ionization energy and the capture cross section of the trap can be deduced from the transient response of the device. In its original form, DLTS was based on the measured change in the capacitance of a p-n junction due to a change in the depletion width caused by electron or hole emission from traps. Other measurements which reflect the emission of free charge carriers from traps can also be used for DLTS. Wessels was one of the first to use current transients to measure deep level traps in a junction diode.⁴ In addition to the characterization of traps in simple junctions, DLTS can be used for the investigation of traps in more complex devices. For example, Sriram and Das have shown the usefulness of current DLTS for characterizing traps in GaAs field effect transistors.⁵

To understand the principle behind DLTS, let us first consider the basic capture and emission processes for deep level traps. The theory for measuring capture and emission rates for trap levels in semiconductors has been described in detail by Sah et al.⁶ Figure 4 is a simple energy band diagram showing the four basic capture and emission processes. Shown in the figure are the valence and conduction band edges E_v and E_c , the shallow level impurities E_a and E_d for shallow acceptor and donor levels, and E_T for the deep level traps. The concentration of electrons in the conduction band is denoted by n . The concentration of holes in the valence band is denoted by p . The concentration of electrons and holes trapped at the impurity centers are n_T and p_T respectively. The four basic processes are denoted by

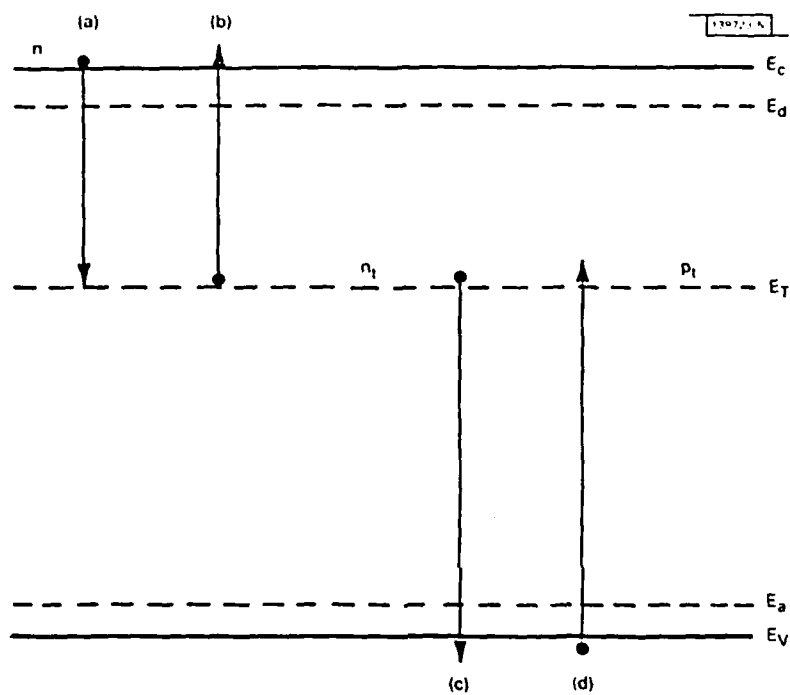


Fig. 4. The four basic capture and emission processes.

a, b, c, and d. Processes a and b involve the capture and emission, respectively, of an electron with the conduction band. Processes c and d are the equivalent capture and emission of a hole with the valence band. The direction of the arrows indicates the movement of electrons. The rate equation describing the population of electrons at the trap level is

$$dn_T/dt = a - b - c + d \quad (1)$$

Let c and e denote capture and emission rates respectively. Let n and p be subscripts to denote electrons and holes respectively. Let N_T represent the total number of traps, and n_T and p_T be the number of trapped electrons and holes, respectively. Since every trap is occupied by either an electron or a hole, $N_T = n_T + p_T$. A capture process depends on the number of unoccupied states in the destination level as well as the number of occupied states in the originating level. Therefore, equation (1) can be written

$$dn_T/dt = c_n n p_T - e_n n_T - c_p p n_T + e_p p_T \quad (2)$$

The steady state occupation of the traps by electrons is given by

$$\begin{aligned} 0 &= c_n n p_T - e_n n_T - c_p p n_T + e_p p_T \\ 0 &= -n_T(c_{pp} + e_n) + (N_T - n_T)(c_{nn} + e_p) \\ n_T &= N_T(c_{nn} + e_p)(c_{pp} + e_n + c_{nn} + e_p)^{-1} \end{aligned} \quad (3)$$

The thermal emission rates of electrons and holes, e_n and e_p respectively, depend upon the temperature and the ionization energy. The ionization energy is the energy separating the trap from the conduction band for electron emission or from the valence band for hole emission. By the principle of detailed balance, the electron emission rate is given by³

$$e_n = \sigma_n v_{th} N_c g_n \exp(-E_i/kT) \quad (4)$$

where σ_n is the electron capture cross section, v_{th} is the electron thermal velocity, $N_c = 2(2\pi m^* kT/h^2)^{3/2}$ is the effective density of states in the

conduction band, g_n is the degeneracy of the trap level and E_i is the ionization energy.

Several of the quantities in equation (4) are temperature dependent. Lang and Logan noted that σ_n may be thermally activated and is of the form, $\sigma_n = \sigma_{n\infty} \exp(-E_b/kT)$.⁷ Mircea et al. showed that the ionization energy varies linearly with temperature and can be expressed in the form, $E_i = E_{i0} - \alpha T$.⁸ The average thermal velocity is temperature dependent, $v_{th} = (3kT/m^*)^{1/2}$. Making these substitutions, equation (4) becomes

$$\begin{aligned} e_n &= 2(2\pi m^* kT/h^2)^{3/2} (3kT/m^*)^{1/2} \sigma_{n\infty} g_n \exp(\alpha/k) \exp[-(E_{i0} + E_b)/kT] \\ &= \gamma_n T^2 \sigma_{na} \exp(-E_{na}/kT) \end{aligned} \quad (5)$$

where γ_n is a constant equal to $2.28 \times 10^{20} \text{ cm}^{-2} \text{ s}^{-1} \text{ K}^{-2}$, $\sigma_{na} = \sigma_{n\infty} g_n \exp(\alpha/k)$, and $E_{na} = E_{i0} + E_b$. E_{na} and σ_{na} are referred to as the apparent ionization energy and the apparent cross section, respectively. A similar equation exists for e_p which includes the terms E_{pa} and σ_{pa} . This form of the emission rate equation was recommended by Martin et al. to facilitate the comparison of DLTS data from different laboratories.⁹

Deep level transient spectroscopy is basically the observation of transients due to the emission of electrons or holes from deep level traps in the depletion region of a p-n junction or metal-semiconductor contact. The transient in the measured quantity is related to the trap emission rate, e_n or e_p . If the transient is measured at various temperatures, this relationship, together with equation (5) for e_n or its counterpart for e_p , can be used to determine E_{na} and σ_{na} or E_{pa} and σ_{pa} . This, in general, is the approach taken for all forms of DLTS.

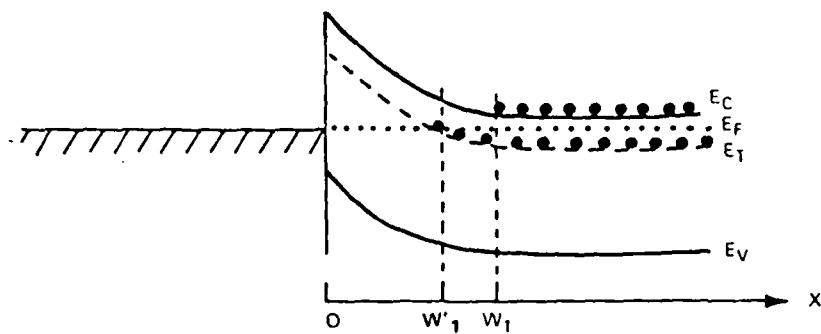
In this investigation of traps in the PBT the transient quantity measured is the collector-emitter current. In Chapter I we briefly examined the principle of operation of the PBT. The collector-emitter current is

controlled by the potential barrier in the base region which the electrons must overcome in order to pass from the emitter to the collector. This potential barrier is governed by the width of the depletion or space-charge region around the base grating due to the metal-semiconductor Schottky contact. The width of the depletion region is determined by, among other things, the concentration of space-charge. The occupation of traps by electrons affects this space-charge concentration and, thus, the depletion width. The emission of electrons or holes from traps within the depletion region around the base grating therefore leads to a transient in the collector-emitter current. The time constant associated with this current is equal to the time constant of the process which empties the traps.

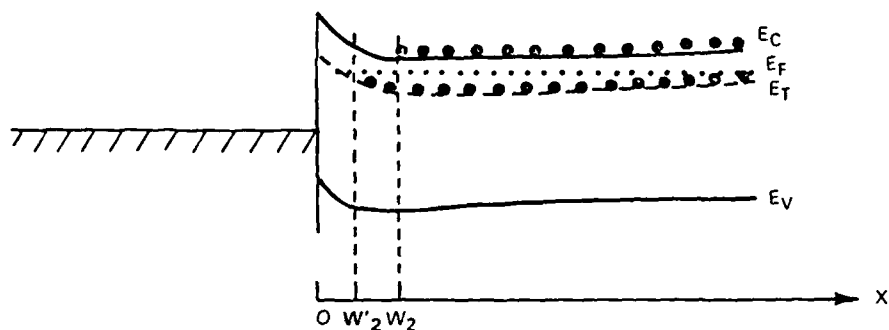
The electron population of a trap level in the depletion region changes due to the emission of both electrons and holes. For this discussion let us consider an n-type semiconductor. Under steady state conditions in the neutral region of the semiconductor the electron capture rate is much greater than the electron emission rate since there are many available electrons, and deep traps tend to remain full. In the depletion region, however, there are few available electrons to be captured, and the traps will be less full, or even mostly empty.

In order to have electrons emitted from traps, the traps must first be filled with electrons. One way to fill the traps in the base region of the PBT is to apply a positive voltage pulse to the base. This is illustrated by the simple band diagrams for a Schottky contact shown in Fig. 5.

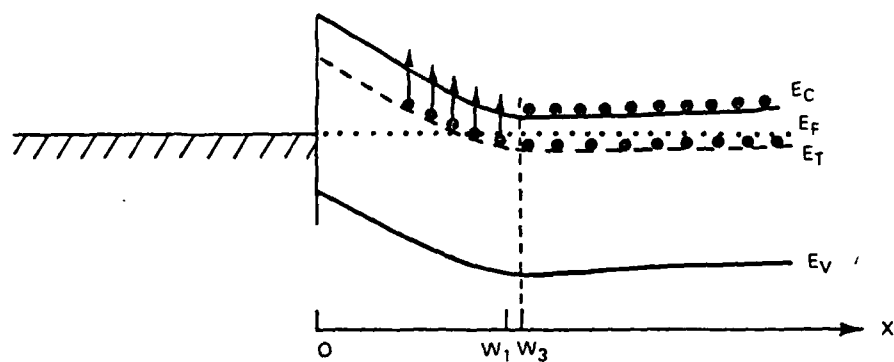
In Fig. 5(a) the Schottky contact is shown under dc bias. The depletion width, W_1 , depends upon the built-in voltage of the Schottky contact, the space charge concentration in the depleted region, and the



(a)



(b)



(c)

Fig. 5. Band diagram for Schottky contact under three bias conditions: (a) constant dc bias; (b) more positive fill-up pulse; and (c) original dc bias immediately after fill-up pulse.

applied bias voltage. As can be seen in the diagram, electron traps up to a depth of W_1' into the depletion region will be empty.

Figure 5(b) shows the Schottky contact after a more positive fill-up pulse has been applied. The larger voltage on the base causes the depletion width to be reduced. The electron traps in the region between W_1' and W_2' become filled because electrons are available to be captured. The hole traps may also capture holes injected from the metal into the semiconductor. A more effective way of filling hole traps is to optically generate electron-hole pairs in the depletion region.

Finally, Fig. 5(c) shows the Schottky contact immediately after the fill-up pulse when the base voltage has returned to its original dc value. The depletion width does not return to its original value, however. The trapped electrons alter the positive space-charge concentration in the depletion region, and the depletion width immediately after the removal of the fill-up pulse is larger than W_1 . As the trapped electrons are emitted, the depletion width returns to its steady state value, W_1 . If holes were trapped, the depletion width would be smaller after the removal of the fill-up pulse, so that the sign of the transient would be reversed.

For DLTS analysis it is assumed that the transient increase or decrease in the depletion width is purely exponential in time. Nonexponential transients may occur for a number of reasons including the spatial variation of the emission rate due to a spatial variation in the junction electric field or the overlapping of the effects of two traps with slightly different emission rates. DLTS analysis still provides useful information for identifying traps although the calculated values of the trap parameters, E_{na} and σ_{na} or E_{pa} and σ_{pa} , may be slightly affected. The effects of nonexponential transients can be detected with DLTS and will be described in

Chapter V. For now, we will assume an exponential transient, i.e., that the depletion width returns to its steady state value after the fill-up pulse at a rate proportional to $\exp(-t/\tau_e)$, where τ_e is either $\tau_n = 1/e_n$ for electron traps or $\tau_p = 1/e_p$ for hole traps.

The collector-emitter current is the quantity measured in these experiments. Since the PBT collector-emitter current depends on the base depletion width, the current transient following the trap fill-up pulse can be used to determine the trap emission rate.

The measurement sequence is illustrated by Fig. 6. It begins with the application of a forward bias pulse to the base which fills the electron traps and perhaps some hole traps in the region around the base grating. After the removal of the fill-up pulse, the collector-emitter current is given by

$$I(t) = I_{ss} + \Delta I(0)\exp(-t/\tau_e) \quad (6)$$

where I_{ss} is the steady state current. If the transient is caused by emission from electron traps, $\Delta I(0)$ is negative. We will define the DLTS signal, $S(T)$, as the difference between the current at time t_1 and at a later time t_2 :

$$S(T) = I(t_1) - I(t_2) \quad (7)$$

Using equation (7) we have

$$S(T) = \Delta I(0)[\exp(-t_1/\tau_e) - \exp(-t_2/\tau_e)] \quad (8)$$

The sign of $S(T)$ distinguishes electron traps from hole traps. The dependence of $S(T)$ on temperature is illustrated in Fig. 7. At low temperatures τ_e is much larger than t_1 and t_2 , the transient is relatively flat over the time period of interest, and $|S(T)|$ is small. As the temperature increases τ_e becomes smaller, and when τ_e is comparable to t_1 and t_2 , $|S(T)|$ becomes relatively large. Finally, as the temperature

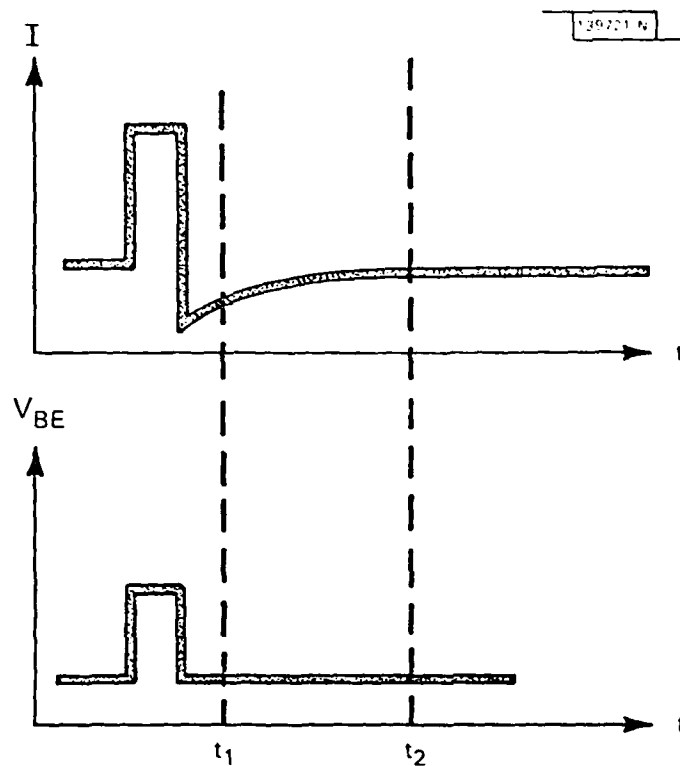


Fig. 6. DLTS measurement sequence.

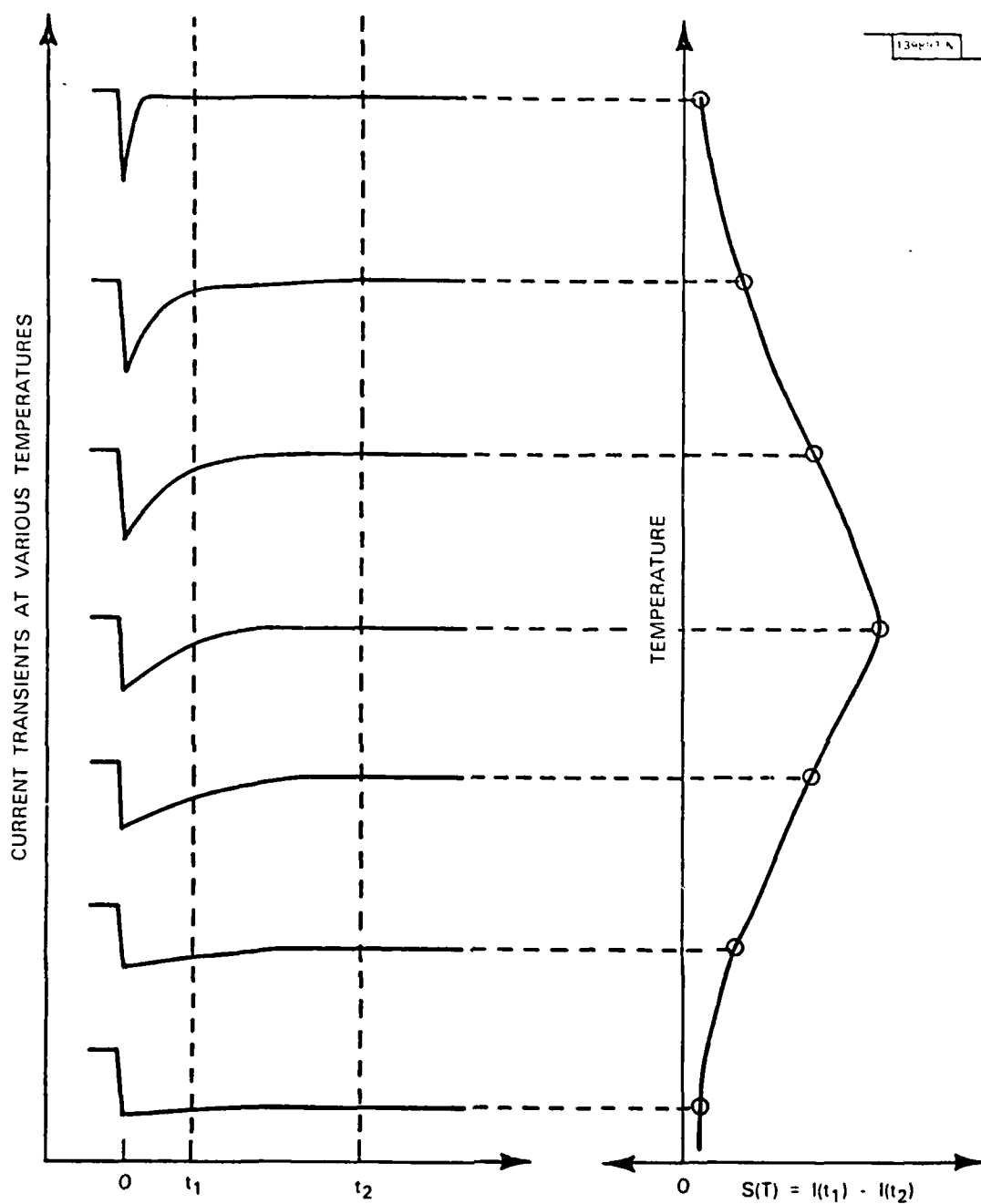


Fig. 7. Dependence of $S(T)$ on temperature.

increases further and τ_e becomes smaller still, the steady state conditions are attained before t_1 , and $|S(T)|$ is again small. Thus, for a given t_1 and t_2 , the magnitude of the DLTS signal, $|S(T)|$, will peak at a characteristic temperature for a given trap level. The τ_e at which this peak occurs can be obtained by maximizing equation (8) with respect to τ_e . We obtain

$$\tau_{\max} = (t_1 - t_2)/\ln(t_1/t_2) \quad (9)$$

The "rate window" is defined as $1/\tau_{\max}$ and is equal to the emission rate at the temperature where the DLTS signal peaks.³ The transient current through the PBT is measured over a range of temperatures, and $S(T)$ versus T is plotted for different values of t_1 and t_2 . At the temperature at which the DLTS signal peaks τ_e , and hence e_n or e_p , can be calculated. For electron traps the resulting values of e_n for different rate windows can be used as points on a $\log(T^2/e_n)$ versus $1000/T$ plot and a straight line can be fitted to these points. The emission rate equation (equation (5)) can be written in the form

$$\log(T^2/e_n) = -\log(\gamma_n \sigma_{na}) + (E_{na}/kT)\log(e) \quad (10)$$

Therefore, E_{na} can be obtained from the slope of the plot, and σ_{na} can be obtained from the y-intercept. A similar plot can be used to determine E_{pa} and σ_{pa} for hole traps.

The apparent electron trap parameters E_{na} and σ_{na} have been measured and reported for many GaAs samples processed under a wide variety of conditions. Martin et al. have tabulated many of the common electron traps in GaAs.⁹ Some of the traps have been identified as chemical impurities, while others are thought to be related to various crystal defects.

One other trap parameter which is of interest and can sometimes be inferred from DLTS data is the trap concentration N_T . For example, the relationship between depletion width and capacitance transients is

sufficiently simple so that N_T can be determined from the capacitance transient if $N_T \ll N_d$. Unfortunately, however, a relationship between the current transients of a PBT and the trap concentration in the PBT has yet to be derived, and the derivation of a reasonably accurate formula based on the current transport properties of the PBT is beyond the scope of this thesis. However, an order-of-magnitude estimate of the trap concentration can be obtained from these DLTS measurements.

To obtain an approximate formula which relates the results of current DLTS measurements to the trap concentration, we can begin by considering a slight change in the number of occupied traps to be equivalent to a slight change in the space charge concentration. Although Bozler and Alley give the results of some numerical simulations of the PBT, the dependence of the collector-emitter current upon donor concentration cannot be derived from these results.¹¹ However, a paper describing further simulations of PBT performance by Marty et al. can be used to obtain an approximate expression for N_T .¹² The results of the simulation include a plot of the collector-emitter current versus the base voltage for several different values of the donor concentration. From this data it was found that the following relationship could be written:

$$\Delta N_d / N_d = a(\Delta I / I) \quad (11)$$

where a is a factor which ranged from 0.4 to 0.7. Relating this to the collector-emitter current from equation (6) immediately after the fill-up pulse when the traps are filled, $|\Delta I| = |\Delta I(0)|$ and $|\Delta N_d| = N_T$. Therefore, a rough approximation of the trap concentration is given by

$$N_T \approx (N_d/2)(|\Delta I(0)|/I) \quad (12)$$

The magnitude of the transient, $|\Delta I(0)|$, can be calculated from the

magnitude of the peak DLTS signal. At the point where $|S(T)|$ is a maximum equation (9) is satisfied. Using this in equation (8) we find

$$|\Delta I(0)| = |S(T_{\text{peak}})| / (K^{-L} - K^{-M}) \quad (13)$$

where $K = t_2/t_1$, $L = 1/(K-1)$, and $M = K/(K-1)$. Therefore, a rough approximation of N_T can be made from the measured DLTS signal and the known value of N_d .

III. MEASUREMENT APPARATUS

The measurement apparatus used in this research is designed to measure and store the transient current through the PBT following a short trap filling pulse applied to the base. The current is sampled at user-selected intervals, averaged over a number of trials, and the value of the current is stored on floppy disk for later analysis of the data. A diagram of the DLTS measurement system is shown in Fig. 8.

System control is provided by a desktop computer. It controls a multiprogrammer over an IEEE 480 interface bus and a temperature controller through a 16-bit binary coded decimal (BCD) interface. A disk drive, a CRT display unit, and a graphics plotter are also interfaced with the computer. Experimental parameters selected by the operator through the computer include trap fill-up pulse height, pulse width, sampling interval, number of samples, number of trials to be averaged, temperature range, and temperature interval. Because of the automated nature of the system, several pulse height parameters can be used during one temperature scan.

The device under test, mounted in a cold chamber, is cooled by a cryocooler. The temperature controller, through the use of a temperature sensor, heater, and feedback electronics, maintains the device at the desired temperature which is sent from the computer through the BCD interface. The temperature is controlled within ± 1 K for measurements at each temperature. The actual temperature of the device is measured with a thermocouple referenced to liquid nitrogen. The temperature range provided by the system is approximately 35 to 400 K.

At each temperature, the transient current following a fill-up pulse is measured. An external power supply provides the collector-emitter bias, and a D/A converter card in the multiprogrammer with a conversion time of 6 μ s

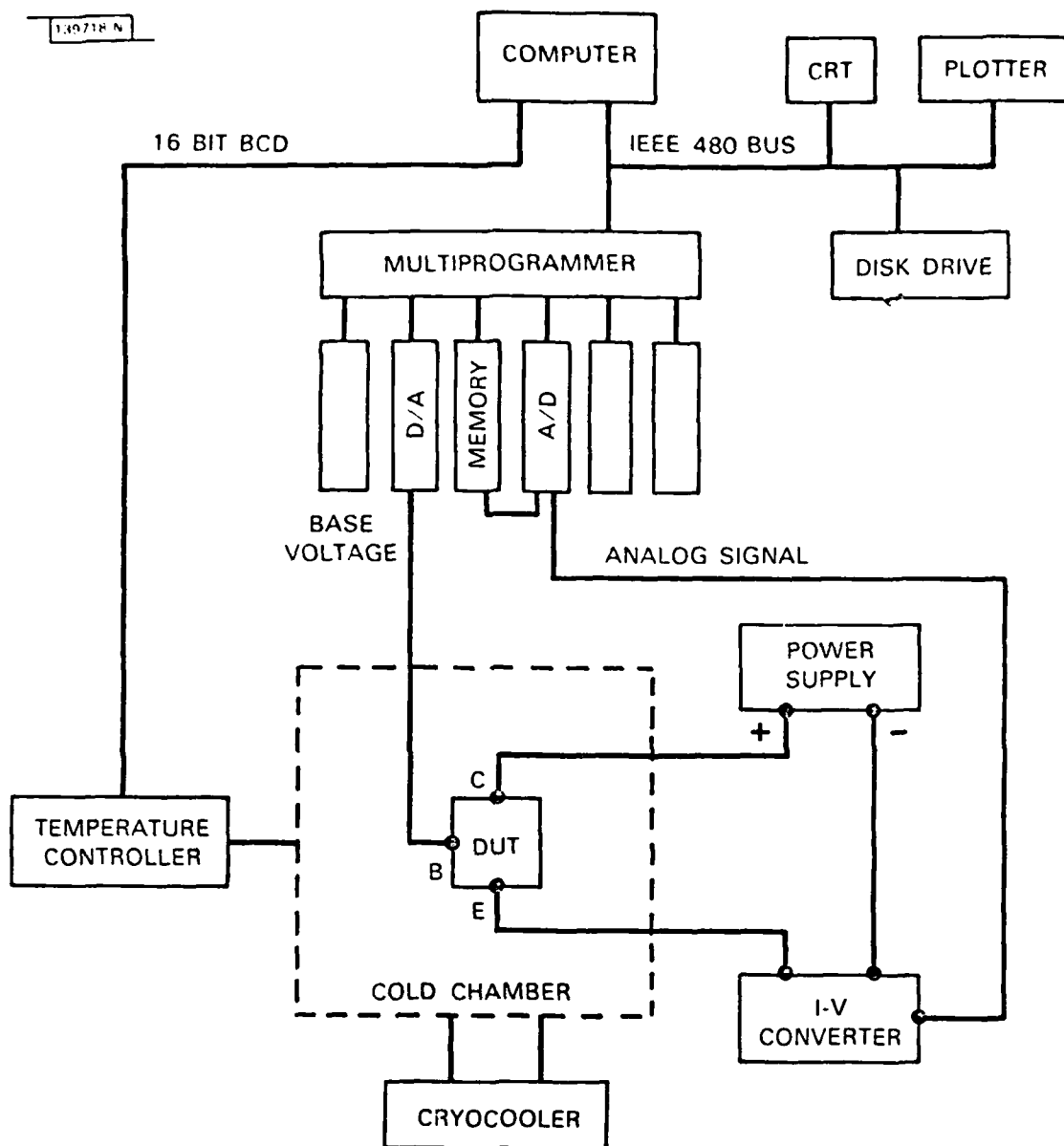


Fig. 8. Diagram of DLTS measurement system.

supplies the required base-emitter bias for the trap fill-up pulse. The base voltage can be maintained within ± 5 mV, and the minimum pulse width is approximately 1.5 ms. If measurements at a number of different pulse height parameters are desired, they are all made before the device is brought to the next temperature.

The collector-emitter current through the PBT is measured by a current-to-voltage converter. The voltage output of the current-to-voltage converter is sampled by an A/D converter card in the multiprogrammer. The sampling interval, minimum 30 μ s, as well as the number of samples, maximum 1024, are selected by the operator. The sampling sequence begins at the end of the fill-up pulse, when the A/D converter is triggered to sample the analog voltage representing the current at the required intervals. The voltage values are stored directly into a memory card in the multiprogrammer. At the end of the sampling sequence, the data are read into the computer. The fill-up pulse and the sampling sequence are repeated for the number of trials desired, and the average value of the current transient is computed. The averaged data values are then stored in a disk file along with other data, such as the temperature, pulse parameters, and sampling time.

Analysis of the stored data is performed after the full temperature scan is completed. Although this can be done in any way desired, the simplest analysis is to select t_1 and t_2 and calculate the difference, $S(T) = I(t_1) - I(t_2)$, in the customary fashion. $S(T)$ is plotted as a function of temperature, and from there the calculation of τ_n or τ_p , E_{na} or E_{pa} , and σ_{na} or σ_{pa} follows the approach outlined in Chapter II. Since the shape of the current transient is stored, other means of determining τ_n or τ_p may be employed. A curve fitting routine may be used to approximate the

exponential functions present in the transient at various temperatures. Whatever the analysis technique, the data are stored, without the necessity of going back to perform more time-consuming measurement scans. With one temperature scan, data for six or more rate windows can usually be obtained, unlike a manual system where each rate window requires a separate temperature scan. Since each temperature scan requires several hours, the practical advantages of this type of system are great.

IV. EXPERIMENTAL RESULTS

The apparent trap parameters E_{na} and σ_{na} or E_{pa} and σ_{pa} have been measured for several GaAs PBT's using the measurement system described in the previous chapter. In this section the measured values of the trap parameters are reported and the significant device fabrication parameters are given. The next chapter discusses the experimental results.

Table 1 provides information about the fabrication parameters used for the devices evaluated in this study. All of the devices were fabricated on heavily doped substrates with an n-type VPE layer as described in Chapter I. There are, however, significant differences in the base metal used. The base metal in Community Chest is tungsten and was deposited by means of argon sputtering. The base metal in Second Chance was also deposited by argon sputtering but consisted of tungsten silicide. The base metal in Johnson II and MP8-3 is tungsten and was deposited by e-beam evaporation in the presence of oxygen. The second epitaxial layer, the overgrowth, was also performed by different epitaxial techniques. The epitaxial growth over the base grating in Second Chance and Community Chest was performed using low temperature VPE. The second epilayer for Johnson II was grown using high temperature VPE, and the epitaxial overgrowth for MP8-3 was achieved using molecular beam epitaxy (MBE). The donor concentration near the interface between these layers was measured on a portion of the wafer next to, but not actually over, the grating area and was approximately 10^{17} cm^{-3} . The actual donor concentration in the region of the grating is not known.

Table 2 lists the devices measured and the traps detected in each device along with the measured trap parameters E_{na} and σ_{na} or E_{pa} and σ_{pa} . Usually, two or three traps in each device were of sufficient magnitude to permit the trap parameters to be determined. In some cases, evidences of

Table 1. Summary of differences in fabrication parameters among PBT's tested.

Device	Type of Base Metal	Base Metallization Method	Overgrowth Method
Second Chance	Tungsten Silicide	Sputtering	Low Temp VPE
Johnson II	Oxygenated Tungsten	e-Beam Evaporation	High Temp VPE
MP8-3	Oxygenated Tungsten	e-Beam Evaporation	MBE
Community Chest	Tungsten	Sputtering	Low Temp VPE

Table 2. Summary of traps detected.

Device	Type of Trap	E_{na}, E_{pa} (eV)	σ_{na}, σ_{pa} (cm ²)	Possible Identity
Second Chance	Electron	0.27	1.4×10^{-16}	EL8
	Electron	0.17	5.1×10^{-16}	EL11
	Hole	0.42	4.9×10^{-15}	HL4
Johnson II	Electron	0.44	8.0×10^{-13}	EL5
	Electron	0.68	1.8×10^{-13}	EL12
MP8-3	Electron	0.47	5.3×10^{-14}	EL4
	Hole	0.55	4.5×10^{-14}	HL8
	Hole	0.44	3.2×10^{-13}	HL4
Community Chest	Electron	0.66	8.0×10^{-12}	EL3
	Hole	0.43	2.1×10^{-14}	HL4

weak traps were detected, but DLTS signal peaks could not be determined with reasonable accuracy. Along with each trap listed in Table 2 are the possible comparisons with traps catalogued by Martin, Mitonneau, and Mircea.^{9,10} Tables 3 and 4 contain the lists of known electron and hole traps. Although none of the electron traps discovered were common to more than one device, one of the hole traps, HL4, was found in three of the four devices.

The four devices listed in Table 2 were all tested using the current DLTS system described in Chapter III. After the data representing the transient current was stored for an appropriate set of temperatures, the DLTS signal, $S(T)$, was computed and plotted as a function of the temperature for various rate windows. An example of such a plot, Fig. 9, shows $S(T)$ versus T for three different rate windows. The steady state voltage was 0.7 V. The base was then pulsed to 1.1 V for a period of 1 ms. The current through the device was measured for a period of 30 ms after the fill-up pulse under a collector-emitter bias of 0.1 V. The data stored on the disk was the average of 100 repetitions of the pulse and measurement sequence.

The next step in determining the trap parameters was to determine at what temperature the DLTS signal peaked for each rate window. This was done manually, and the accuracy of the determination was related to the smoothness of the $S(T)$ versus T curve. To reduce the effect of measurement errors, six rate windows were usually used to measure each trap, and the corresponding six peak temperatures were recorded.

From these values of the rate windows and the peak temperatures, the electron trap parameters E_{na} and σ_{na} were calculated using the procedure described in Chapter II. Least squares fits to the $\log(T^2/e_n)$ versus $1000/T$ plots were determined with the computer and graphics plotter. The

Table 3. Parameters E_{na} and σ_{na} for known electron traps. This table is from reference 9.

Label	Activation Energy, E_{na} (eV)	Emission Cross Section, σ_{na} (cm ²)	Observations
ET1	0.85	6.5×10^{-13}	Bulk material
ET2	0.30	2.5×10^{-15}	Bulk material
ES1	0.83	1.0×10^{-13}	Bulk material
EF1	0.72	7.7×10^{-15}	Cr doped bulk mat.
EI1	0.43	7.3×10^{-16}	V.P.E. mat.
EI2	0.19	1.1×10^{-14}	V.P.E. mat.
EI3	0.18	2.2×10^{-14}	V.P.E. mat.
EB1	0.86	3.5×10^{-14}	Cr doped L.P.E. mat.
EB2	0.83	2.2×10^{-13}	As grown V.P.E. mat.
EB3	0.90	3.0×10^{-11}	Electron irradiated mat.
EB4	0.71	8.3×10^{-13}	Electron irradiated mat.
EB5	0.48	2.6×10^{-13}	As grown M.B.E. mat.
EB6	0.41	2.6×10^{-13}	Electron irradiated mat.
EB7	0.30	1.7×10^{-14}	As grown M.B.E. mat.
EB8	0.19	1.5×10^{-14}	As grown M.B.E. mat.
EB9	0.18	Imprecise	Electron irradiated mat.
EB10	0.12	Imprecise	Electron irradiated mat.
EL1	0.78	1.0×10^{-14}	Cr doped bulk mat.
EL2	0.825	$(0.8-1.7) \times 10^{-13}$	V.P.E. mat.
EL3	0.575	$(0.8-1.7) \times 10^{-13}$	V.P.E. mat.
EL4	0.51	1.0×10^{-12}	As grown M.B.E. mat.
EL5	0.42	$(0.5-2.0) \times 10^{-13}$	V.P.E. mat.
EL6	0.35	1.5×10^{-13}	Bulk material
EL7	0.30	7.2×10^{-15}	As grown M.B.E. mat.
EL8	0.275	7.7×10^{-15}	V.P.E. mat.
EL9	0.225	6.8×10^{-15}	V.P.E. mat.
EL10	0.17	1.8×10^{-15}	As grown M.B.E. mat.
EL11	0.17	3.0×10^{-16}	V.P.E. mat.
EL12	0.78	4.9×10^{-12}	V.P.E. mat.
EL14	0.215	5.2×10^{-16}	Bulk material
EL15	0.15	5.7×10^{-13}	Electron irradiated mat.
EL16	0.37	4.0×10^{-18}	V.P.E. mat.

Possible Comparisons

EL2 = ET1 = ES1 = EB2
 EL4 = EB5
 EL5 = EB6(?)
 EL6 = ET2

EL7 = EB7; EL7 = EL6(?)
 EL11 = EI3 = EL10(?)
 EL12 = EB4(?)
 EL15 = EB9

Table 4. Parameters E_{pa} and σ_{pa} for known hole traps. This table is from reference 10.

Label	Activation Energy, E_{pa} (eV)	Emission Cross Section, σ_{pa} (cm ²)	Observations
HT1	0.44	1.2×10^{-14}	V.P.E. mat.
HS1	0.58	2.0×10^{-19}	L.P.E. mat.
HS2	0.64	4.1×10^{-16}	L.P.E. mat.
HS3	0.44	4.8×10^{-18}	L.P.E. mat.
HB1	0.78	5.2×10^{-16}	Cr doped L.P.E. mat.
HB2	0.71	1.2×10^{-14}	As grown L.P.E. mat.
HB3	0.52	3.4×10^{-16}	Fe doped L.P.E. mat.
HB4	0.44	3.4×10^{-14}	Cu doped L.P.E. mat.
HB5	0.40	2.2×10^{-13}	As grown L.P.E. mat.
HB6	0.29	2.0×10^{-14}	Electron irradiated L.P.E.
HL1	0.94	3.7×10^{-14}	Cr doped V.P.E. mat.
HL2	0.73	1.9×10^{-14}	As grown L.P.E. mat.
HL3	0.59	3.0×10^{-15}	Fe diffused V.P.E. mat.
HL4	0.42	3.0×10^{-15}	Cu diffused V.P.E. mat.
HL5	0.41	9.0×10^{-14}	As grown L.P.E. mat.
HL6	0.32	5.6×10^{-14}	V.P.E. with p ⁺ layer
HL7	0.35	6.4×10^{-15}	As grown M.B.E. mat.
HL8	0.52	3.5×10^{-16}	As grown M.B.E. mat.
HL9	0.69	1.1×10^{-13}	As grown V.P.E. mat.
HL10	0.83	1.7×10^{-13}	As grown V.P.E. mat.
HL11	0.35	1.4×10^{-15}	Melt grown mat.
HL12	0.27	1.3×10^{-14}	Zn contaminated L.P.E.

Possible Comparisons

HL1 = HB1 = HS1
 HL2 = HB2 = HS2
 HL3 \approx HL8
 HL4 = HB4 = HT1

HL5 = HB5
 HL7 = HB6(?)
 HL8 = HB3
 HL11 = HL5(?)

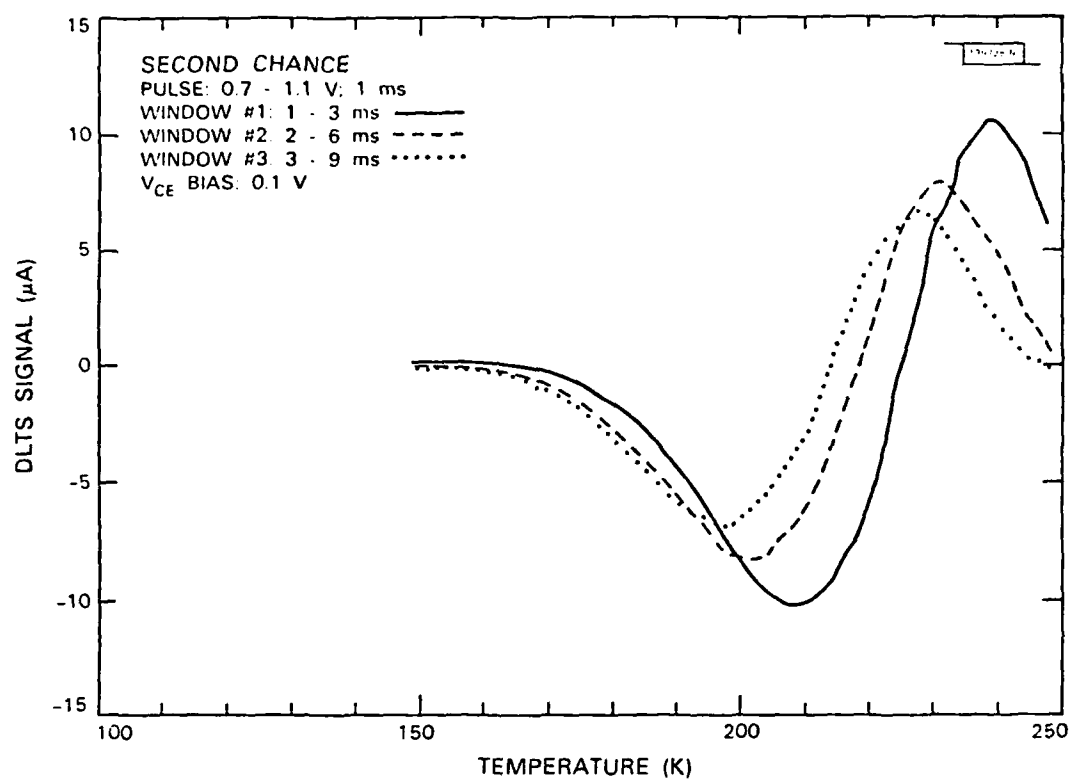


Fig. 9. Example of DLTS signal versus temperature.

correlation coefficient for the fit was usually better than 0.99. Figure 10 shows the $\log(T^2/e_n)$ versus $1000/T$ plots for two electron traps detected and two known traps. Although the values of E_{na} (0.68 eV and 0.66 eV) and σ_{na} ($1.8 \times 10^{-13} \text{ cm}^2$ and $8.0 \times 10^{-12} \text{ cm}^2$) for the two traps are fairly close, it is apparent from the plots of the known traps that one of the measured traps is closer to EL3 and the other is closer to EL12. The best way to identify traps, therefore, is to compare the plotted values of the traps with those of known traps rather than to compare only the numerical values of E_{na} and σ_{na} .

One obvious source of error in the calculation of E_{na} and σ_{na} is the determination of the temperatures at which $S(T)$ peaks. It was found that a difference of 1 K in one of the six peak temperatures resulted in approximately a 3% change in E_{na} and approximately a 40% change in σ_{na} . If all of the peak temperatures were shifted by 1 K, E_{na} changed by less than 1% and σ_{na} changed by approximately 9%. Depending on the smoothness of the $S(T)$ versus T plot, the location of the signal peaks could usually be determined to within 2-4 K with fairly high confidence. As discussed above, however, the most useful information for identifying traps is the $\log(T^2/e_n)$ versus $1000/T$ plot rather than the numerical values of the trap parameters themselves.

Besides the trap parameters E_{na} and σ_{na} , the trap concentration, N_T , was calculated. As explained in Chapter II, any number obtained for the trap concentration is just a rough approximation and depends upon the accuracy of the estimate for N_d . In addition, the estimated value of N_T is actually a lower limit, since there may only be a partial change in occupancy of the trap level during the forward bias pulse. Table 5 lists

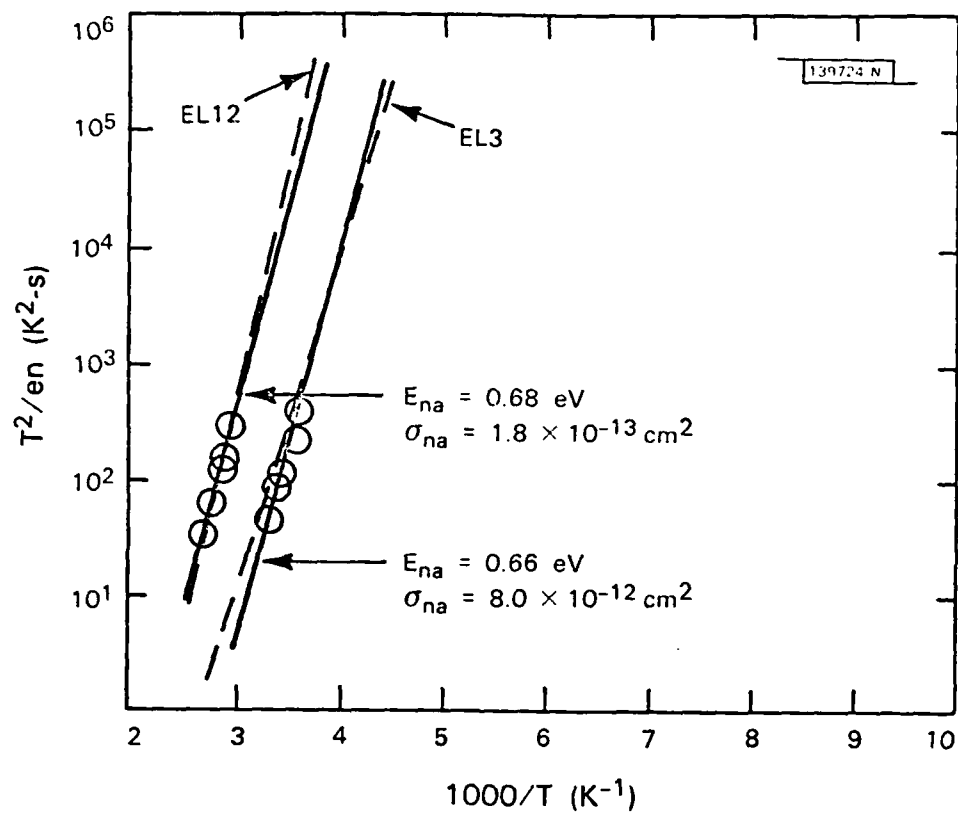


Fig. 10. Plots for two measured traps (solid lines) and two known traps (dashed lines). The data points are shown by circles.

Table 5. Approximate trap concentrations.

Device	Trap	$ S(T_{\text{peak}}) $ (μA)	$ \Delta I(0) $ (μA)	I (μA)	Estimated N_T (cm^{-3})
Second Chance	EL8	14.0	36.4	119	1.5×10^{16}
	EL11	0.25	0.65	9.8	3.3×10^{15}
	HL4	11.0	28.6	216	6.6×10^{15}
Johnson II	EL5	2.3	4.3	148	1.5×10^{15}
	EL12	6.5	12.1	310	2.0×10^{15}
MP8-3	EL4	0.8	1.5	43	1.7×10^{15}
	HL8	4.2	7.8	210	1.9×10^{15}
	HL4	3.8	7.1	73	4.8×10^{15}
Community Chest	EL3	5.0	9.3	229	2.0×10^{15}
	HL4	60.0	112	463	1.2×10^{16}

the values of $|\Delta I(0)|$ and I at several of the DLTS signal peaks and gives the estimate of N_T for several of the traps detected.

Again referring to Fig. 9, we see that there is a positive peak as well as a negative peak in the DLTS signal plot. The positive peak, indicating a hole trap, was unexpected, but hole traps were detected in three of the devices tested. In the DLTS literature the voltage pulse method of filling minority carrier traps is usually considered ineffective in Schottky barrier junctions because the number of injected holes is usually very small. Optical generation of electron-hole pairs is usually used in order to observe minority carrier traps in such junctions. For capacitance DLTS the level of forward bias permitted is very small and too few holes are injected to fill hole traps. However, in the current DLTS experiments performed in this research the level of forward bias during the trap fill-up pulse was sometimes around 1 V, and an adequate number of holes could be injected. For one of the devices tested, Community Chest, a forward voltage of 1 V during the fill-up pulse resulted in a hole trap being indicated, while a forward voltage of 0.4 V did not allow this trap to be seen.

Although some hole traps were observed, the trap filling mechanism was not as efficient for some hole traps as for electron traps. The effect of the fill-up pulse width on the DLTS signal from the hole trap in Second Chance was studied. Figure 11 illustrates the increase in the amplitude of the hole trap peak as the fill-up pulse width was increased from 10 μ s to 1 ms. The hole trap peak did not increase as the pulse width was increased further to 10 ms, which indicates a capture rate of the order of 10^3 s^{-1} . The emission rate for this hole trap was measured to be $5.5 \times 10^{-2} \text{ s}^{-1}$. Since this trap at 0.42 eV above the valence band is below the quasi-Fermi level for holes, the capture rate should be nearly equal to the emission

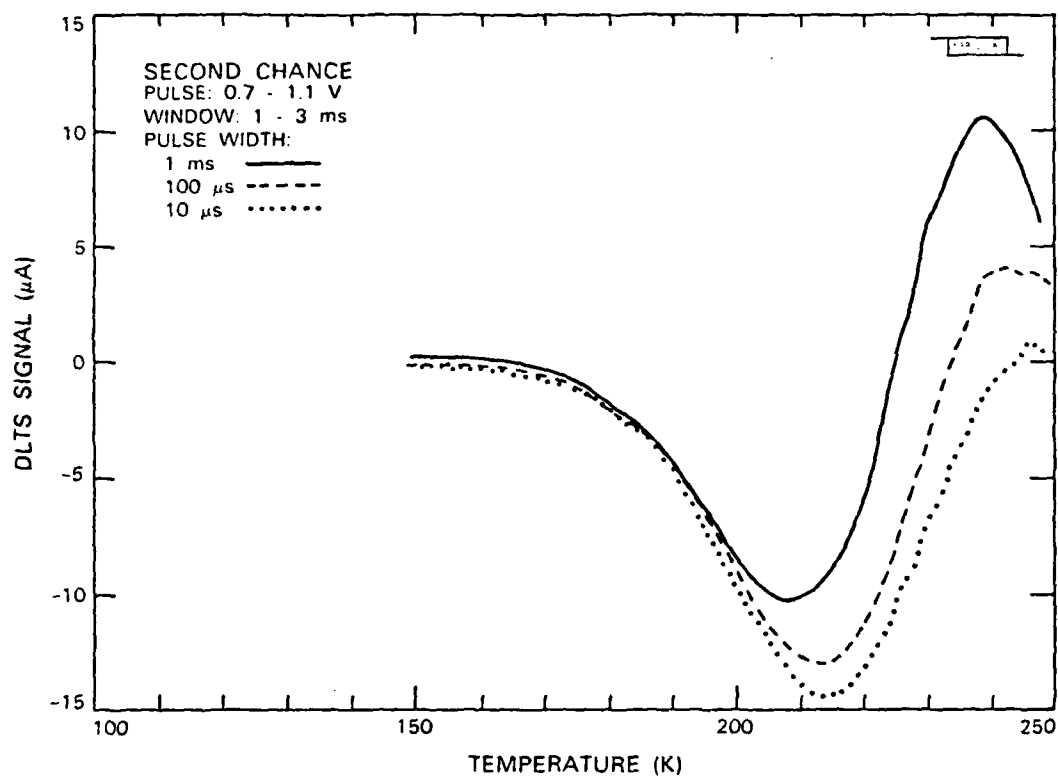


Fig. 11. Dependence of hole trap peak height on fill-up pulse width.

rate. Therefore, the capture rate determined from varying the pulse width is consistent with the value of e_{pa} calculated from DLTS.

Figure 11 also shows that the amplitude of the electron trap peak decreased as the fill-up pulse width increased. This can be explained by considering the addition of the transients due to the electron trap and the hole trap. Since the emission rates of the hole trap and the electron trap are relatively close to each other, as the amplitude of the hole trap transient increases due to the increase in the pulse width, this transient, opposite in polarity from the electron trap transient, partially offsets the electron trap transient and decreases the DLTS signal.

This chapter briefly summarizes the electron and hole traps detected in several PBT devices. Except for one of the hole traps different traps were detected in each device. This may be due to the fact that each device was fabricated slightly differently. The measurement of the DLTS signal peaks introduces some error in the values calculated for E_{na} and σ_{na} or E_{pa} and σ_{pa} , but the traps observed can usually be identified relative to known traps by comparing plots of the measured data with plots of known traps. Although the voltage pulse method of filling traps is not usually used for observing minority carrier traps in Schottky barrier junctions, the level of forward bias used in these experiments allowed hole traps as well as electron traps to be seen.

V. DISCUSSION

Probably the most important type of information one would like to obtain from DLTS is the identity of the chemical impurity or crystal defect detected within the sample. Although DLTS has been utilized for approximately ten years and deep levels have been studied much longer than that, very few traps have been positively associated with specific defects or impurities. Instead, traps in GaAs are commonly known only by a system of letters and numbers established by Martin, Mitonneau, and Mircea.^{9,10}

One problem associated with linking traps to specific causes is that the "trap signature" E_{na} and σ_{na} or E_{pa} and σ_{pa} are only the apparent ionization energy and capture cross section and do not correspond to any real physical quantities. As was mentioned in Chapter II, the true ionization energy of a trap varies with temperature. In addition, the true capture cross section is thermally activated. The precise corrections to the apparent trap parameters necessary to obtain E_t and σ_n or σ_p are not always known.

Another difficulty involved in obtaining the true trap parameters is the effect of high electric fields on trap emission. In his original paper on DLTS, Lang noted that spatial variations in the electric field could lead to nonexponential transients and a change in DLTS peak location and shape with a change in junction bias conditions.³ This is due to the fact that traps in different areas of the device experience different values of the electric field and have different emission rates. The emission rate observed by DLTS is, therefore, an average of all the emission rates in a given region. A study was made by Makram-Ebeid on the effect of an electric field on the trap EL2 in GaAs.¹³ The emission rate was observed first to decrease and then to increase as the junction electric field was increased.

Although the behavior of other electron traps may not be the same as that of EL2, a high junction field can have a significant impact on the trap emission rate and, thus, the apparent trap parameters.

Unfortunately, the strength of the junction electric field in the base region of the PBT is not precisely known. The simple calculation of the electric field for a planar Schottky barrier with carrier concentrations and bias levels typical of a PBT gives a maximum field strength of the order of 10^5 V/cm. However, because of the sharp edges and corners around the base grating, the local electric field could be considerably higher in that region. Changes in the base voltage would change the local electric field and could alter the measured values of E_{na} and σ_{na} or E_{pa} and σ_{pa} .

Evidence was found in the data for a dependence of the measured value of σ_{na} on the junction electric field. Table 6 lists some DLTS data obtained from Second Chance under three different base bias conditions. As can be seen, as the steady state voltage on the base increased, the DLTS peak shifted to a lower temperature, and the calculated value for σ_{na} increased. It is conceivable that the three peaks could correspond to different traps since different regions of the device are sampled with different fill-up pulse parameters. However, the fact that the values of E_{na} for all the peaks are nearly the same seems to indicate that the same trap is responsible for all of them. A change in the apparent cross section with a change in base voltage was also observed for the hole trap discovered in MP8-3. Even though the junction electric field can alter the values of the trap parameters, measured traps can usually be identified by comparing the $\log(T^2/e_n)$ versus $1000/T$ plots of the measured traps with those of known traps.

Table 6. Change in DLTS peak location as base bias changed for Second Chance. Rate window: $5.49 \times 10^2 \text{ sec}^{-1}$.

Steady State Voltage (V)	Pulse Voltage (V)	Temperature of DLTS Peak (K)	E_{na} (eV)	σ_{na} (cm ²)
0.5	0.9	242	0.30	8.8×10^{-17}
0.6	1.0	228	0.31	4.0×10^{-16}
0.7	1.1	214	0.27	1.4×10^{-16}

Table 2 also includes the possible identification of the traps discovered in this research. Most of the known traps have not yet been associated with specific chemical impurities or crystal defects, but there are exceptions. The hole trap HL8 is thought to be due to iron and was detected in MP8-3. The hole trap HL4 has been related to copper and was found in MP8-3, Community Chest, and Second Chance. Some recent studies by Hollis at Lincoln Laboratory indicate that there may be significant amounts of these elements in the base metal of some devices.¹⁴ The concentration of various elements in a tungsten film deposited on GaAs was measured using secondary ion mass spectrometry (SIMS). In an oxygenated evaporated tungsten film, similar to the base metal in MP8-3, the peak concentration of iron was $7 \times 10^{19} \text{ cm}^{-3}$ and the peak concentration of copper was $2 \times 10^{19} \text{ cm}^{-3}$. In a sputtered tungsten film, deposited in a way similar to that of Community Chest and Second Chance, the copper concentration was also $2 \times 10^{19} \text{ cm}^{-3}$, but the iron concentration was much less, $5 \times 10^{17} \text{ cm}^{-3}$. The base metal of Johnson II is also oxygenated evaporated tungsten, but it was deposited several years ago. SIMS analysis of tungsten films from the same period shows a relatively low level of impurities.

Another experiment using SIMS analysis indicated that the copper present in the tungsten tended to diffuse into the GaAs during device fabrication. The experiment involved the normal fabrication of a PBT with a sputtered tungsten base up to the point of the epitaxial growth over the base grating. In this "stop action" experiment the grating was only partially overgrown, filling in the spaces between the grating lines. The tungsten was etched away after the overgrowth and another VPE layer was grown on the homogeneous surface which resulted. A SIMS depth profile detected copper in a region around the base grating with a peak

concentration of around $8 \times 10^{17} \text{ cm}^{-3}$. The width of the region where copper was found, about 4000 Å, indicated significant diffusion of copper out of the metal grating. This experiment shows that the hole trap HL4 found in Second Chance and Community Chest could be due to the presence of copper in the base grating and its diffusion into the semiconductor during subsequent fabrication steps.

A similar stop action experiment using an oxygenated evaporated tungsten base, similar to that in MP8-3, has not yet been performed. Since the concentration of copper in this type of base metal is also relatively high, it is plausible that the same sort of copper diffusion into the semiconductor occurred. It is not known whether the same sort of diffusion of iron out of the metal occurs, but it is a possible explanation for the presence of the trap HL8.

The concentration of copper in the GaAs determined by SIMS is considerably higher than that estimated through DLTS. One reason for this discrepancy could be that the peak concentration detected by SIMS was in the immediate vicinity of the base metal. The region of the device sampled by DLTS depends upon the fill-up pulse voltages and may have been further away from the base metal where the copper concentration was lower. Another reason for a lower concentration estimated by DLTS is that perhaps not all the copper atoms were acting as hole traps. Copper in GaAs, in fact, has four different energy levels within the band gap, one of which is observable as HL4.

Although most of the traps discovered in the PBT's tested cannot be linked to specific causes, current DLTS still provides some very useful information. The number of traps observed and their approximate concentrations can be helpful to those involved in designing and fabricating

future PBT's. If a larger number of PBT's are tested, some traps common to most of them may be observed as well as other traps not discovered in this research. A systematic study of PBT fabrication parameters and their effect on deep level traps observed could be very useful in identifying ways to improve device performance. The research described in this thesis is only the first step in a potentially very important study of deep level traps in the GaAs PBT.

VI. SUMMARY

The purpose of the research described in this thesis was to investigate deep level electron traps in the GaAs PBT using current DLTS. In the introduction to this thesis the major characteristics of the PBT were described. Because deep level traps in the base region of the PBT could have an effect on device performance, current DLTS was used to measure these traps, since the collector-emitter current is very sensitive to trap activity in that region.

In Chapter II the DLTS technique was described. DLTS involves the measurement of the transient response of a p-n or metal-semiconductor junction due to the emission of electrons or holes from deep level traps within the depletion region. In this case, an exponential transient in the collector-emitter current corresponds to the emission of electrons or holes from traps within the depletion region around the base grating of the PBT. The time constant associated with this transient can be deduced from DLTS thermal scans, and the apparent ionization energy and capture cross section of traps can be calculated.

Chapters III and IV described the current DLTS measurement apparatus and presented the results of measurements made on several PBT devices. An attempt was made to associate the traps observed with some traps that have been observed in other laboratories.

Finally, Chapter V discussed the extent to which the deep level traps observed can be associated with specific chemical impurities or crystal defects. The calculated values of E_{na} and σ_{na} or E_{pa} and σ_{pa} can be affected by the junction electric field. In spite of this, measured traps can usually be identified relative to known traps. One of the traps observed, HL4, is thought to be due to copper and was found in three of the

devices. A different hole trap found in one of the devices is thought to be due to iron. Another study using SIMS analysis seems to corroborate the DLTS data obtained in this research. Even though the precise nature of most traps is unknown, current DLTS promises to be a useful tool for studying the PBT by characterizing deep level traps in the active region of the device.

REFERENCES

1. G. L. Miller, D. V. Lang, and L. C. Kimerling, "Capacitance Transient Spectroscopy," in Annu. Rev. Mater. Sci., vol. 7, R. H. Bube, and R. W. Roberts, Eds. Palo Alto: Annual Reviews, 1977, pp. 391-448.
2. C. O. Bozler, G. D. Alley, R. A. Murphy, D. C. Flanders, and W. T. Lindley, "Fabrication and Microwave Performance of the Permeable Base Transistor," in IEDM Tech. Dig., pp. 384-387, 1979.
3. D. V. Lang, "Deep Level Transient Spectroscopy: A New Method to Characterize Traps in Semiconductors," J. Appl. Phys., vol. 45, pp. 3023-3032, 1974.
4. B. W. Wessels, "Determination of Deep Levels in Cu-Doped GaP Using Transient-Current Spectroscopy," J. Appl. Phys., vol. 47, pp. 1131-1133, 1976.
5. S. Sriram and M. B. Das, "Characterization of Electron Traps in Ion-Implanted GaAs MESFET's on Undoped and Cr-Doped LEC Semi-Insulating Substrates," IEEE Trans. Electron Devices, vol. ED-30, pp. 586-592, 1983.
6. C. T. Sah, L. Forbes, L. L. Rosier, and A. F. Tasch, Jr., "Thermal and Optical Emission and Capture Rates and Cross Sections of Electrons and Holes at Imperfection Centers in Semiconductors from Photo and Dark Junction Current and Capacitance Experiments," Solid-State Electron. vol. 13, pp. 759-788, 1970.
7. D. V. Lang and R. A. Logan, "A Study of Deep Levels in GaAs by Capacitance Spectroscopy," J. Electron. Mater., vol. 4, pp. 1053-1066, 1975.
8. A. Mircea, A. Mitonneau, and J. Vannimenus, "Temperature Dependence of Ionization Energies of Deep Bound States in Semiconductors," J. Phys. (Lett.) (Paris), vol. 38, pp. L41-L43, 1977.
9. G. M. Martin, A. Mitonneau, and A. Mircea, "Electron Traps in Bulk and Epitaxial GaAs Crystals," Electron. Lett., vol. 13, pp. 191-192, 1977.
10. A. Mitonneau, G. M. Martin, and A. Mircea, "Hole Traps in Bulk and Epitaxial GaAs Crystals," Electron. Lett., vol. 13, pp. 666-667, 1977.
11. C. O. Bozler and G. D. Alley, "Fabrication and Numerical Simulation of the Permeable Base Transistor," IEEE Trans. Electron Devices, vol. ED-27, pp. 1128-1144, 1980.
12. A. Marty, J. Clarac, J. P. Bailbe, and G. Rey, "Two-Dimensional Finite-Element Simulation of a Permeable-Base Transistor," IEE Proc., vol. 130, pp. 24-28, 1983.

13. S. Makram-Ebeid, "Effect of Electric Field and Current Injection on the Main Electron Trap in Bulk GaAs," Proc. M. R. S. Symposia, vol. 2, pp. 497-501, 1981.
14. M. A. Hollis, private communication.